

Supplemental material

Lee et al., <https://doi.org/10.1084/jem.20182313>

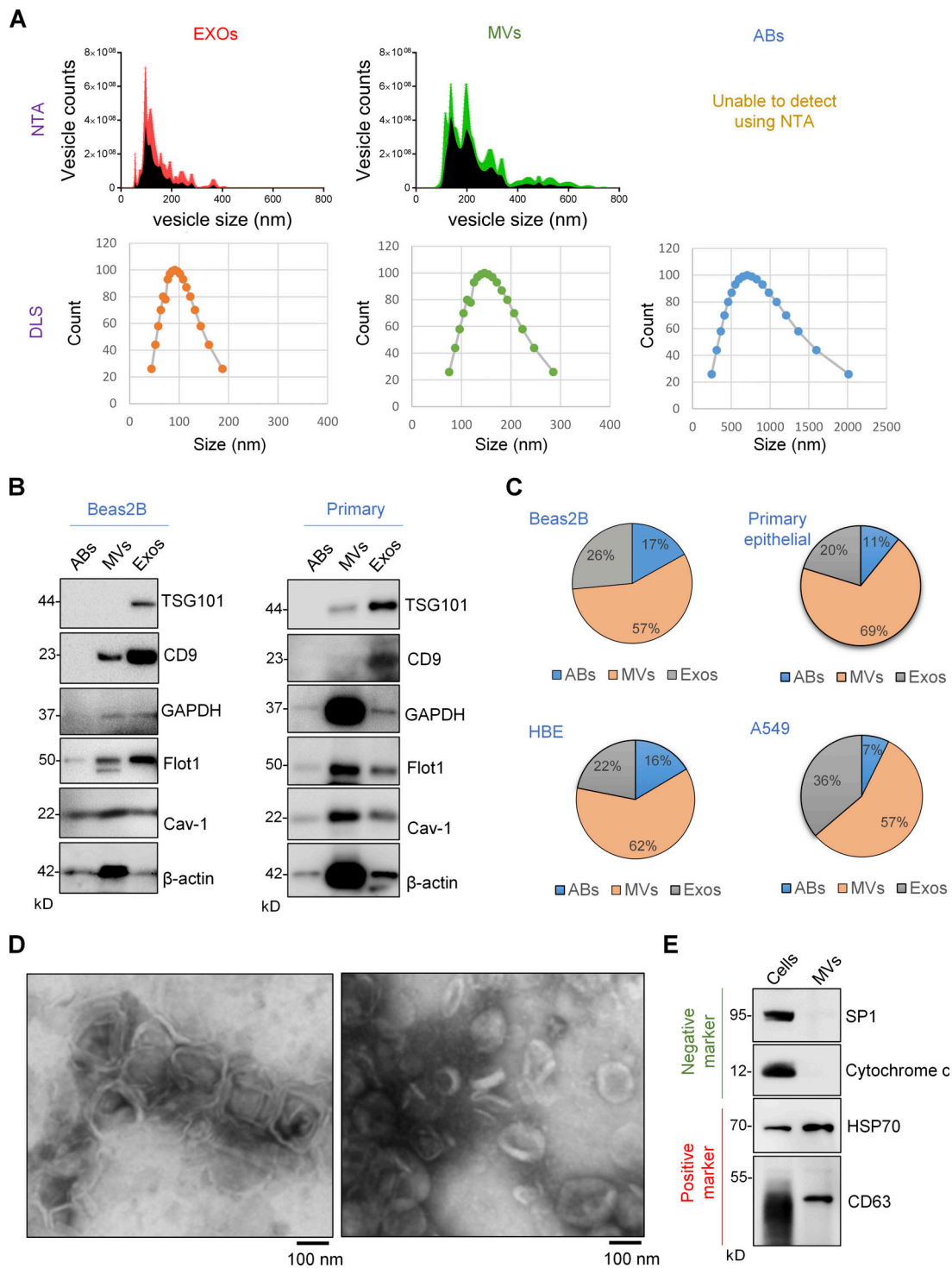


Figure S1. **Characterizations of three subpopulations of EVs.** (A–C) Three types of EVs (ABs, MVs, and Exos) were isolated from lung epithelial cells (Beas2B, mouse primary, HBE, or A549 cells). EV sizes were characterized using NTA and DLS (A). EV marker proteins were determined using Western blots with indicated antibodies (B). Average protein percentages of each type of EVs ( $n = 3$ ). (D and E) Morphology and purity of the MVs isolated from Beas2B cells were evaluated using TEM (D) and Western blots (E). The data are representative of two independent experiments (A) or are from three independent experiments (C). The Western blots (B and E) and TEM images (D) are representative of two independent experiments.

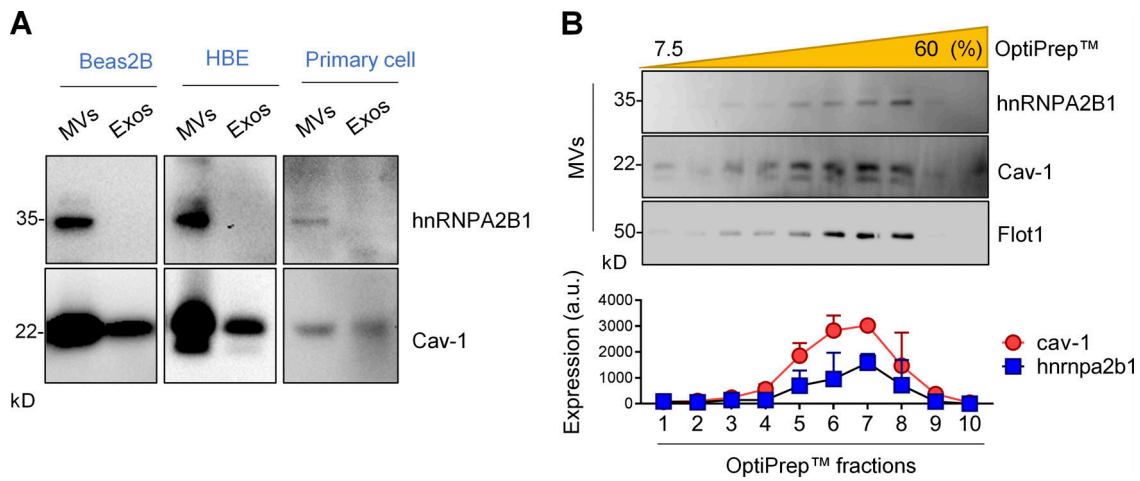


Figure S2. **HnRNA2B1 expressions in MVs and Exos derived from lung epithelial cells. (A and B)** MVs and Exos were isolated from Beas2B, HBE, and mouse primary lung epithelial cells under hyperoxia conditions. HnRNA2B1 and cav-1 were detected using Western blot (A). The isolated hyperoxic MVs were subjected to iodixanol density gradient fractionation, followed by Western blot with indicated antibodies. The Western blots are representative of two (A) and three (B) independent experiments. a.u., arbitrary units.

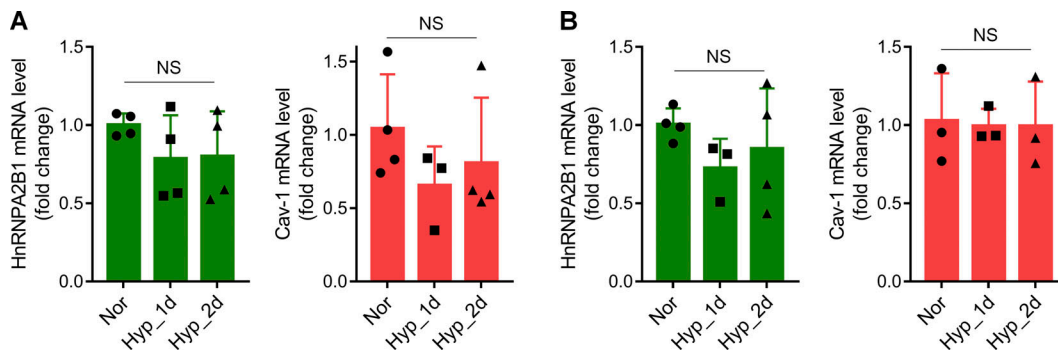
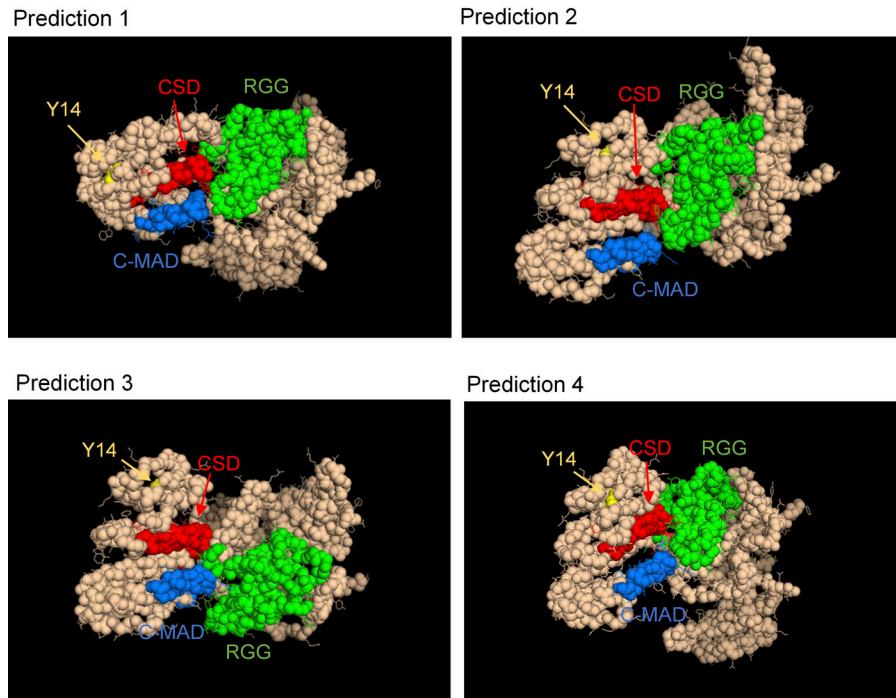


Figure S3. **mRNA expressions of cav-1 and hnRNA2B1 in lung epithelial cells. (A and B)** Human Beas2B (A) and mouse primary lung epithelial cells (B) were exposed to hyperoxia (Hyp). mRNA levels of cav-1 and hnRNA2B1 were then determined using qPCR. The data are from three independent experiments with different cell batches. Nor, normoxia.

**A**  
I-TASSER-based interaction models



**B**  
Interaction residue prediction

Modeling	Interaction residue (hnRNP2B1)					Interaction residue (Caveolin-1)				
		F195	F196	F215		Y97	W98	F99		
Prediction 1		F195	F196	F215		Y97	W98	F99		
Prediction 2		F195		F215	Y264	Y97	W98	F99		
Prediction 3	N194	F195				Y97		F99	R146	Y148
Prediction 4		F195	F196	F215	Y264	Y97	W98	F99	R146	Y148

Figure S4. **I-TASSER**-based interaction models between *cav-1* and *hnRNP2B1*. **(A)** Putative 3D structural models of the *cav-1*/*hnRNP2B1* complex were constructed using I-TASSER. **(B)** Docking sites between *cav-1* and *hnRNP2B1* were then analyzed based on the four I-TASSER predictions.

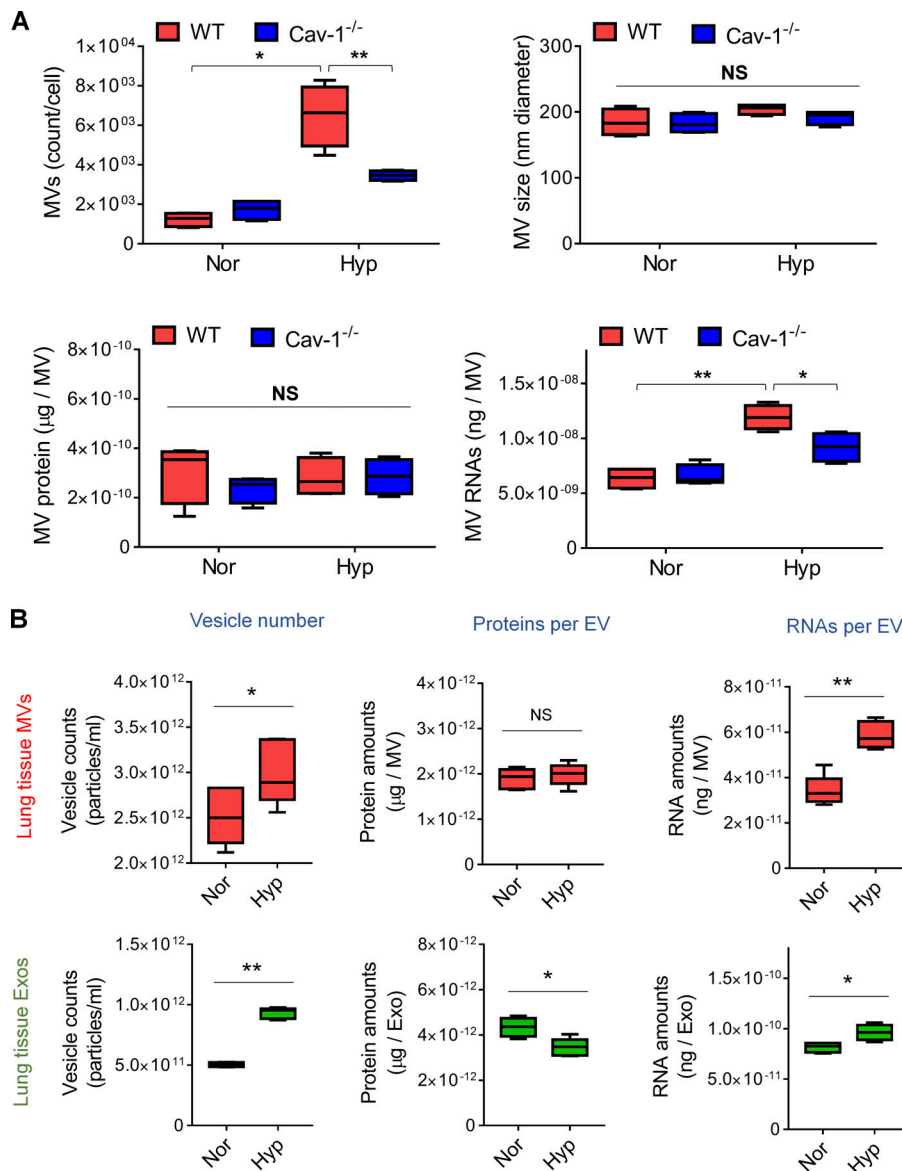


Figure S5. **Characterization of EVs from lung epithelial cells and lung tissue under hyperoxia condition.** (A and B) EVs (MVs or Exos) were isolated from WT and cav-1<sup>-/-</sup> epithelial cells (A) or mouse lung tissues (B) under normoxia (Nor) or hyperoxia (Hyp) conditions. EV count, EV size, protein level per EV, and RNA level per EV were evaluated using NTA, Bradford assay, and Nanodrop. The data are from three independent experiments. \*, P < 0.05; \*\*, P < 0.01 between the groups indicated.

Table S1–S5 are provided as a single Excel file. Table S1 shows the miRNA expression levels presented in Fig. 1 F. Table S2 shows the miRNA expression levels presented in Fig. 2, B and C. Table S3 shows the copy number of miR-17/93 in lung epithelial MVs. Table S4 shows the gene expressions presented in Fig. 8 L. Table S5 shows the material information.